# Density functionals: Where do they come from, why do they work?

Matthias Ernzerhof, John P. Perdew, and Kieron Burke
*Department of Physics and Quantum Theory Group, Tulane University, New Orleans, LA 70118*
(To appear in *Density Functional Theory*, ed. R. Nalewajski, Springer-Verlag, Berlin, 1996*)

Gradient-corrected or semi-local functionals (GGA's) have achieved the accuracy required to make density functional theory a useful tool in quantum chemistry. We show that local (LSD) and semi-local functionals work because they usefully model the exchange-correlation hole around an average electron, rather than by yielding accurate results at all electron positions. We discuss the system-averaged hole at small interelectronic separations, where such functionals are extremely accurate, and at large interelectronic separations, where the local approximation is incorrect for finite systems. We argue that the "on-top" hole density provides the missing link between real atoms and molecules and the uniform electron gas. We show how exchange-correlation potentials can be related to energies. We also discuss how the degree of nonlocality, i.e., the error made by LSD, is related to the spatial extent of the hole. Decomposing the energy by coupling-constant and spin, we find that the deeper the on-top hole is, the smaller the error in the local approximation to the energy. We use this insight to demonstrate that Hartree-Fock hybrid functionals do not consistently improve on GGA. A different hybrid invokes wavefunction methods for exchange and parallel-spin correlation, but we show that configuration interaction wavefunction calculations with limited basis sets for the Ne atom make the same relative errors in the antiparallel- and parallel-spin correlation energies, despite the lack of a Coulomb cusp in the parallel-spin correlation hole. Finally, we review a recent reinterpretation of spin density functional theory, which is preferable to the standard interpretation in certain cases of extreme nonlocality.

71.10.+x, 71.45.Gm, 31.20.Sy

## I. DENSITY FUNCTIONALS IN QUANTUM CHEMISTRY AND SOLID STATE PHYSICS: INTRODUCTION AND SUMMARY

Most practical electronic structure calculations using density functional theory [1] involve solving the Kohn-Sham equations [2]. The only unknown quantity in a Kohn-Sham spin-density functional calculation is the exchange-correlation energy (and its functional derivative) [2]

$$E_{\rm XC} = T - T_{\rm S} + V_{ee} - U, \qquad (1)$$

where $T$ is the interacting kinetic energy, $T_{\rm S}$ is the non-interacting kinetic energy, $V_{ee}$ is the exact Coulomb repulsion, and $U = \int d^3r \int d^3r' n(\mathbf{r})\, n(\mathbf{r}')/2|\mathbf{r}-\mathbf{r}'|$ is the classical Coulomb energy associated with the density $n(\mathbf{r})$. Modern density functional calculations are based on some approximate form of $E_{\rm XC}$. For example, the local spin density (LSD) approximation [2] is:

$$E_{\rm XC}^{\rm LSD}[n_\uparrow, n_\downarrow] = \int d^3r\; n(\mathbf{r})\; \epsilon_{\rm XC}^{\rm unif}\big(n_\uparrow(\mathbf{r}), n_\downarrow(\mathbf{r})\big), \qquad (2)$$

where $\epsilon_{\rm XC}^{\rm unif}\big(n_\uparrow(\mathbf{r}), n_\downarrow(\mathbf{r})\big)$ is the exchange-correlation energy per particle of a uniform electron gas (jellium) [3,4]. Eq. 2 is exact for an electron gas of uniform (jellium) or slowly-varying spin densities.

For many years, LSD has been very popular with solid-state physicists [1], and quite unpopular with quantum chemists [5]. LSD achieves a remarkable moderate accuracy for the energies and densities of almost all systems, no matter how rapidly their densities vary. In fact, LSD solid-state calculations are often called *ab initio*. However, this moderate accuracy is insufficient for chemical purposes, and no way was known to improve the approximation systematically.

Recently, a new class of functionals, called generalized gradient approximations (GGA's) [6–14], has been developed. These take the general form

$$E_{\rm XC}^{\rm GGA}[n_\uparrow, n_\downarrow] = \int d^3r\; f(n_\uparrow(\mathbf{r}), n_\downarrow(\mathbf{r}), \nabla n_\uparrow, \nabla n_\downarrow), \qquad (3)$$

where the function $f$ is chosen by some set of criteria. The idea is that, by including information about the gradient, one should be able to improve the accuracy of the functional. Several forms for $f$ are currently in use in the literature [7–11], but we focus on the Perdew-Wang 1991 (PW91) form [11–14], because it is derived without semiempirical parameters and is the 'best' functional on formal grounds [12]. Results of calculations with this form show that it typically reduces exchange energy errors from 10% in LSD to 1% and correlation energy errors from 100% to about 10% [13]. PW91 corrects the LSD overestimate of atomization energies for molecules and solids in almost all cases, it enlarges equilibrium bond lengths and lattice spacings, usually correctly, and reduces vibrational frequencies and bulk moduli, again usually correctly [14]. PW91 also generally improves activation barriers [15] and yields an improved description of the phase diagram of Fe under normal or high pressure [16]. In almost all cases where PW91 has been carefully tested, it significantly improves on LSD. Thus

PW91 and similar GGA's have become popular in quantum chemistry.

The success of PW91 can be understood in terms of its construction as a systematic, parameter-free refinement of LSD. While LSD does not typically work well at all points in the system (section II A), it does remarkably well for system-averaged quantities, such as the energy, because the average electron lives in a region of moderate density variation and because the LSD exchange-correlation hole satisfies many conditions satisfied by the exact hole. A straightforward gradient expansion violates these conditions, but a real-space cutoff procedure restores them [8,11], leading to an improved description of system-averaged quantities, as shown in section II B. The PW91 functional is a parametrization of the result of this procedure. In particular, we study the system-averaged exchange-correlation hole, a function of the separation between any two points in the system, and demonstrate that LSD gives a remarkably accurate description of this quantity [17], which is improved by PW91 [17].

The LSD and PW91-GGA system-averaged holes agree at zero interelectronic separation, where both are nearly exact. In section II C, we discuss how the near-universality of this "on-top" hole density provides the missing link between real atoms and molecules and the uniform electron gas. Except very close to the nucleus, the *local* on-top hole density is also accurately represented by LSD, even in the classically-forbidden tail region of the electron density [18].

In Ref. [12], Perdew and Burke made a graphical comparison of various GGA's. The popular functionals for exchange (Perdew-Wang 86 [8], Becke 88 [9], and Perdew-Wang 91 [11–14]) are similar for practical purposes, but the popular functionals for correlation are not. In particular, the Lee-Yang-Parr 88 [10] functional is rather different from the Perdew-Wang 1986 [7], and 1991 [11–14] correlation functionals. In fact, the LYP correlation energy is in error by about a factor of two in the important uniform-gas limit [18]. We discuss this difference further in section II D, as we believe it has important consequences for the description of delocalized electrons in carbon clusters and metals, and for spin-magnetized systems. Indeed, because PW91 is the "most local" [12] of the GGA's for exchange and correlation, as defined in section III, it is the least likely to overcorrect the subtle LSD errors for solids.

While the LSD exchange-correlation hole is accurate for small interelectronic separations (section II C), it is less satisfactory at large separations, as discussed in section II E. For example, consider the hole for an electron which has wandered out into the classically-forbidden tail region around an atom (or molecule). The exact hole remains localized around the nucleus, and in section II E we give explicit results for its limiting form as the electron moves far away [19]. The LSD hole, however, becomes more and more diffuse as the density at the electron's position gets smaller, and so is quite incorrect. The weighted density approximation (WDA) and the self-interaction correction (SIC) both yield more accurate (but not exact) descriptions of this phenomenon.

PW91 and other GGA's significantly improve the exchange-correlation energy, but the corresponding potential $v_{\rm XC} = \delta E_{\rm XC}/\delta n(\mathbf{r})$ is *not* much improved over LSD, and is in some respects worse [20–22]. We address this point in detail in section II F. From our perspective, this is neither a surprising nor disturbing result. We are fitting a "square peg" (the exact $E_{\rm XC}[n_\uparrow, n_\downarrow]$ with its derivative discontinuities [23,24]) into a "round hole" (the simple continuum approximation of Eq. 3). The areas (integrated properties) of a square and circle can be matched, but their perimeters (differential properties) remain stubbornly different. (For completeness, we note that the potential $v_{\rm XC}(\mathbf{r})$, a functional derivative, can also be constructed from a more physical perspective [25–29]).

While PW91 and other GGA's are more accurate than LSD, another factor-of-five reduction in error is needed to reach chemical accuracy. This might be achieved by isolating those aspects of the exchange-correlation problem that local and semi-local approximations treat well, and using more nonlocal approaches for the remainder. To do this, we must first understand the origin of nonlocal effects, i.e., corrections to LSD, in the energy (section III). Because LSD works best in the vicinity of the electron, the shorter the range of the hole, the better it is described by local and semi-local approximations [18]. Furthermore, because of sum-rules satisfied by both the exact hole and its functional approximation, the deeper the on-top hole is, the shorter is its range. Thus the depth of the on-top hole is strongly related to how accurate LSD (and, by extension, PW91) energies are.

This kind of analysis is relevant to the hybrid functionals which mix exact Hartree-Fock with semi-local functionals and are currently popular [30,31]. The exchange on-top hole is shallower than the exchange-correlation hole, and so the exchange energy is less local than exchange and correlation together. Thus GGA's might be improved by mixing some exact Hartree-Fock exchange. However, we show in section III B that the optimum amount of mixing is far from universal.

Another possible hybrid approach combines a density functional for antiparallel-spin correlation with conventional wavefunction methods for exchange and parallel-spin correlation. The parallel-spin correlation has no on-top hole density, and so is less local than the entire correlation energy, as we show in section III C. This hybrid approach thus relies on the fact that the antiparallel-spin correlation can be accurately described by a local or semilocal density functional, and on the hope that the parallel-spin correlation contribution can be easily calculated within a finite basis-set approach such as the coupled-cluster (CC) or configuration-interaction (CI) techniques. Finite basis-set methods are known to be inefficient in describing the antiparallel-spin Coulomb cusp (see, e.g., [32–34]), and are believed to be efficient in the description of the more long-ranged parallel-

spin correlation hole [35]. However, we show that, within the range of computationally-tractable basis sets, the convergence rates of the parallel and antiparallel-spin contributions to the correlation energy are comparable.

So far we have not distinguished between the self-consistent spin densities and the exact ones, because in most systems the difference is slight. In section IV, we discuss 'abnormal' systems, where the self-consistent spin magnetization density, $m(\mathbf{r}) = n_\uparrow(\mathbf{r}) - n_\downarrow(\mathbf{r})$, is very different from the exact spin density. In such systems LSD (and PW91) functionals, evaluated on the exact spin densities, give very poor energies, but these functionals perform much better self-consistently. A stereotypical example is the stretched $H_2$ molecule, which has $m(\mathbf{r}) = 0$ everywhere. The LSD self-consistent solution makes the molecule (incorrectly) magnetized, with an $\uparrow$ electron on one nucleus, and a $\downarrow$ electron on the other. We review a re-interpretation of the standard theory [36], which shows that in such systems, it is in fact the on-top pair density which is well-approximated (i.e., differs little from its exact value) in LSD and GGA calculations for these systems, rather than $m(\mathbf{r})$. In the absence of an external magnetic field, the spin magnetization density is therefore *not* as robust a prediction as the energy and the density itself.

We use atomic units throughout ($e^2 = \hbar = m = 1$), unless otherwise stated.

## II. EXCHANGE-CORRELATION HOLE

In order to understand why approximate functionals yield accurate exchange-correlation energies, we decompose the exchange-correlation energy as follows [37]. We define the pair density of the inhomogeneous system as

$$P_\lambda(\mathbf{r},\mathbf{r}') = N(N-1)\sum_{\sigma_1,\ldots,\sigma_N}\int d^3r_3\ \ldots\int d^3r_N \times\left|\Psi_\lambda(\mathbf{r},\sigma_1,\mathbf{r}',\sigma_2,\ldots,\mathbf{r}_N,\sigma_N)\right|^2, \qquad (4)$$

where $N$ is the number of electrons in the system, $\mathbf{r}_i,\sigma_i$ are the spatial and spin coordinates of the $i$th electron, and $\Psi_\lambda$ is the ground-state wavefunction of the system in which the strength of the Coulomb repulsion is given by $\lambda e^2$, where $0 \le \lambda \le 1$, and in which the external potential varies with $\lambda$, $v_{\sigma,\lambda}(\mathbf{r})$, in such a way as to keep the spin densities $n_\sigma(\mathbf{r})$ fixed [38]. The expectation value of the electron-electron repulsion operator is defined here as

$$V_{ee,\lambda} = \int d^3r\ \int d^3r'\ \frac{P_\lambda(\mathbf{r},\mathbf{r}')}{2|\mathbf{r}-\mathbf{r}'|}. \qquad (5)$$

The exchange-correlation hole density at $\mathbf{r}'$ around an electron at $\mathbf{r}$ for coupling strength $\lambda$, $n_{\mathrm{XC},\lambda}(\mathbf{r},\mathbf{r}')$, is then defined by the relation

$$P_\lambda(\mathbf{r},\mathbf{r}') = n(\mathbf{r})\ \big(n(\mathbf{r}') + n_{\mathrm{XC},\lambda}(\mathbf{r},\mathbf{r}')\big), \qquad (6)$$

where $n(\mathbf{r})$ is the density at $\mathbf{r}$. We may define an exchange-correlation energy as a function of coupling strength $\lambda$ as simply $1/2$ the Coulomb attraction between the $\lambda$-dependent hole density and the density of the electron it surrounds, i.e.,

$$E_{\mathrm{XC},\lambda} = V_{ee,\lambda} - U = \frac{1}{2}\int d^3r\ \int d^3r'\ \frac{n(\mathbf{r})\ n_{\mathrm{XC},\lambda}(\mathbf{r},\mathbf{r}')}{|\mathbf{r}-\mathbf{r}'|}. \qquad (7)$$

Note that this definition of $E_{\mathrm{XC},\lambda}$ differs from others, e.g. Ref. [39], but is convenient for the present purpose.

By defining all these quantities as explicit functions of $\lambda$, we can relate the density functional quantities to those more familiar from quantum chemistry. The exchange-correlation energy of density functional theory can be shown, via the Hellmann-Feynman theorem [38,37], to be given by a coupling-constant average, i.e.,

$$E_{\mathrm{XC}} = \int_0^1 d\lambda\ E_{\mathrm{XC},\lambda}. \qquad (8)$$

(Note that, in the absence of explicit $\lambda$-dependence, our notation implies the coupling-constant averaged quantity.) On the other hand, at full coupling strength, $\lambda = 1$, we return to the fully-interacting system, so that, from Eqs. 6 and 7,

$$E_{\mathrm{XC},\lambda=1} = V_{ee,\lambda=1} - U = E_{\mathrm{XC}} - T_{\mathrm{C}}, \qquad (9)$$

where $T_{\mathrm{C}} = T - T_{\mathrm{S}}$ is the correlation contribution to the kinetic energy. At zero coupling strength ($\lambda = 0$), the system is the non-interacting Kohn-Sham system, i.e., $v_{\sigma,\lambda=0}$ is the Kohn-Sham potential, and only exchange effects remain,

$$E_{\mathrm{XC},\lambda=0} = E_{\mathrm{X}}. \qquad (10)$$

We do not distinguish here this density functional definition of exchange energy from that of Hartree-Fock (HF). This simplification is well-justified, if the HF electron density and the exact electron density differ only slightly [40]. Similarly, the coupling-constant averaged exchange-correlation hole is the usual one referred to in density functional theory, while the full coupling-strength hole can be extracted from the exact interacting wavefunction, via Eqs. 4 and 6, and the exchange hole is that of the non-interacting Kohn-Sham wavefunction $\Psi_{\lambda=0}$. For purposes of comparison between exact quantities calculated with more accurate methods and density functional quantities, we typically use the $\lambda = 0$ and $\lambda = 1$ contributions, which can be extracted directly from the Hartree-Fock and accurate interacting wavefunctions, respectively, whose details are given in appendix A. We obtain the density functional approximations to such quantities by undoing the coupling-constant integration in the functional definitions.

The approach that we take to the question of how local and semilocal density functionals work for systems with large

density gradients was pioneered by Gunnarsson, Jonson, and Lundqvist [41,42]. Define $\mathbf{u} = \mathbf{r}' - \mathbf{r}$, the separation of two points in the system. Then the spherically-averaged hole is

$$n_{\mathrm{XC},\lambda}(\mathbf{r}, u) = \int \frac{d\Omega_u}{4\pi}\; n_{\mathrm{XC},\lambda}(\mathbf{r}, \mathbf{r}+\mathbf{u}). \qquad (11)$$

By studying the exchange (i.e.,$\lambda = 0$) hole in Ne, Gunnarson et al. pointed out that the LSD approximation to this quantity was far better than the LSD approximation to the exchange hole prior to spherical-averaging. Then, from Eq. 7, the energy depends only on this spherically-averaged hole, i.e.,

$$E_{\mathrm{XC},\lambda} = \int_0^\infty du\; 2\pi u \int d^3r\; n(\mathbf{r})\; n_{\mathrm{XC},\lambda}(\mathbf{r}, u). \qquad (12)$$

In the subsections below, we show how this idea has been refined by further study of the exchange-correlation hole since that work.

### A. Point-wise decomposition of energy

A natural way to decompose the exchange-correlation energy is in terms of the exchange-correlation energy per particle. Half the electrostatic potential at $\mathbf{r}$ due to the density of the hole surrounding an electron at $\mathbf{r}$ is

$$\begin{aligned}\epsilon_{\mathrm{XC},\lambda}(\mathbf{r}) &= \int d^3r'\; \frac{n_{\mathrm{XC},\lambda}(\mathbf{r}, \mathbf{r}')}{2|\mathbf{r}-\mathbf{r}'|} \\ &= \int_0^\infty du\; 2\pi u\; n_{\mathrm{XC},\lambda}(\mathbf{r}, u), \end{aligned} \qquad (13)$$

and we take this as our definition of the exchange-correlation energy per particle. While other definitions are also possible, this definition is unambiguous, since $n_{\mathrm{XC},\lambda}(\mathbf{r}, \mathbf{r}')$ is defined in terms of the pair density, Eq. 6. Then LSD may be considered as making the approximation $\epsilon_{\mathrm{XC},\lambda}(\mathbf{r}) = \epsilon^{\mathrm{unif}}_{\mathrm{XC},\lambda}\big(n_\uparrow(\mathbf{r}), n_\downarrow(\mathbf{r})\big)$. In Figs. 1 and 2, we plot $\epsilon_{\mathrm{X}}(\mathbf{r}) = \epsilon_{\mathrm{XC},\lambda=0}(\mathbf{r})$ and $\epsilon_{\mathrm{C},\lambda=1}(\mathbf{r}) = \epsilon_{\mathrm{XC},\lambda=1}(\mathbf{r}) - \epsilon_{\mathrm{X}}(\mathbf{r})$ for the He atom, both exactly and in LSD. We see that the LSD curves are not very accurate. LSD yields the wrong value at $r = 0$ (where $\nabla^2 n/n^{5/3}$ diverges), has an incorrect cusp at $r = 0$, and decays exponentially as $r \to \infty$ (where $|\nabla n|/n^{4/3}$ diverges). The He atom is particularly difficult for LSD, because of the relative importance of the "rapidly-varying" regions $r \to 0$ and $r \to \infty$. However, the radial density-weighted curve, shown for the exchange energy in Fig. 3, looks much better. The LSD errors at small and large $r$ are given little weight. The LSD approximation to the density-weighted integral of these curves, $E_{\mathrm{XC},\lambda} = \int d^3r\; n(\mathbf{r})\; \epsilon_{\mathrm{XC},\lambda}(\mathbf{r})$, is only in error by 16% at $\lambda = 0$ and by 6% at $\lambda = 1$, as can be seen in Table I. (Note that we do not plot any PW91 curves, because PW91 invokes an integration by parts over $\mathbf{r}$, and so makes meaningful predictions only for system-averaged quantities.) We

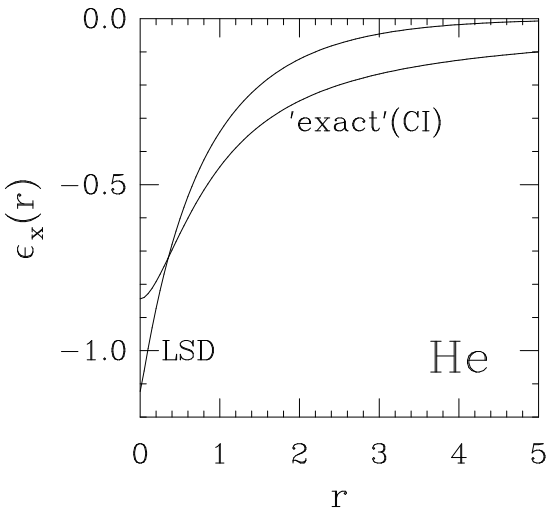


FIG. 1. Exchange energy per electron in the He atom, both exactly (CI) and in LSD. The nucleus is at $r = 0$.

conclude that, while the spherically-averaged hole is better in LSD than the unaveraged hole, it is vital to consider density-weighted quantities to understand their effect on the corresponding total energy.

Similar remarks may be made about the exchange-correlation potential, $v_{\mathrm{XC}}(\mathbf{r}) = \delta E_{\mathrm{XC}}/\delta n(\mathbf{r})$, which, for the He atom, is shown very accurately in Figs. 10 and 11 of Ref. [21]. An important piece of $v_{\mathrm{XC}}(\mathbf{r})$ is $2\epsilon_{\mathrm{XC}}(\mathbf{r})$. Again,

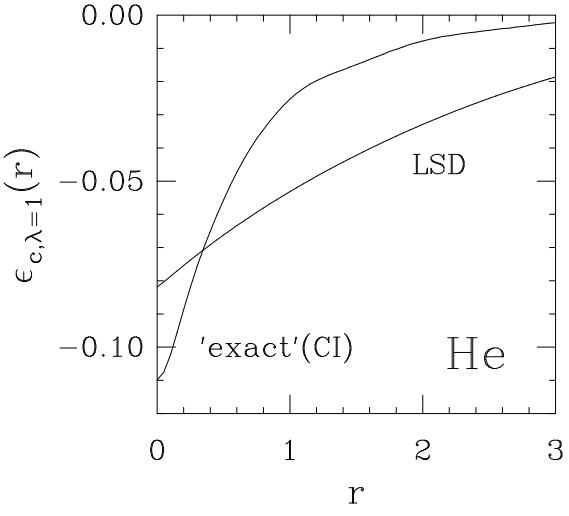


FIG. 2. Correlation energy per electron at full coupling-strength in the He atom, both exactly (CI) and in LSD. The nucleus is at $r = 0$.

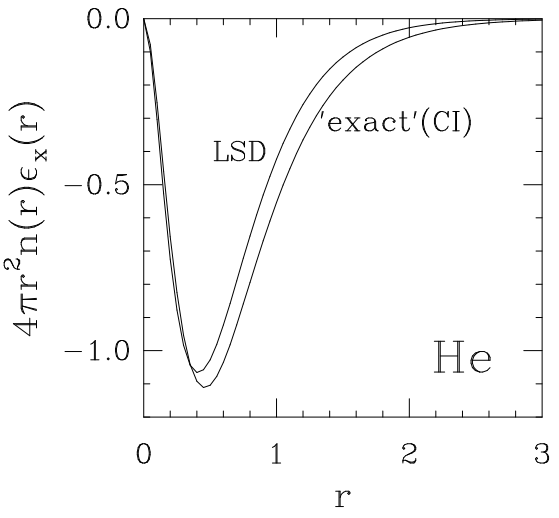


FIG. 3. Exchange energy per electron times the radial density in the He atom, both exactly (CI) and in LSD. The area under each curve is the exchange energy.

LSD is inaccurate at small $r$ and large $r$. In fact, PW91 is even worse, having a divergence at small $r$. It has been pointed out that the PW91 correlation potential would look closer to the exact potential if its sign were reversed! But, as in the case of the energy per particle, it is unclear what the effect of a poor-looking potential is on the quality of the energy. We show in section II F how a different decomposition yields more insight into which properties are being well-approximated by LSD and PW91.

TABLE I. Various energies of the He atom (in eV). The approximate energies were evaluated on the self-consistent densities, and their errors measured relative to the exact energies. All numbers taken from Table III of Ref. [19]. (1 hartree = 27.2116 eV.)

| Energy | LSD | error | PW91 | error | Exact |
|---|---|---|---|---|---|
| $E_{\rm X}$ | -23.449 | (-16%) | -27.470 | (-1%) | -27.880 |
| $E_{\rm C}$ | -3.023 | (164%) | -1.224 | (7%) | -1.146 |
| $T_{\rm C}$ | 1.825 | (83%) | 1.010 | (1%) | 0.997 |
| $E_{\rm XC}$ | -26.472 | (-9%) | -28.693 | (-1%) | -29.026 |
| $E_{{\rm XC},\lambda=1}$ | -28.297 | (-6%) | -29.704 | (-1%) | -30.023 |
| $E_{\rm C}+T_{\rm C}$ | -1.198 | (705%) | -0.213 | (43%) | -0.149 |

### B. Real-space decomposition of energy

The real-space decomposition of the energy is in terms of $\mathbf{u}=\mathbf{r}'-\mathbf{r}$, the separation between points in the system [43]. We define the system- and angle-averaged hole as

$$\langle n_{{\rm XC},\lambda}(u)\rangle = \int \frac{d\Omega_u}{4\pi}\,\frac{1}{N}\int d^3r\; n(\mathbf{r})\; n_{{\rm XC},\lambda}(\mathbf{r},\mathbf{r}+\mathbf{u})$$

$$= \frac{1}{N}\int d^3r\; n(\mathbf{r})\; n_{{\rm XC},\lambda}(\mathbf{r},u), \qquad (14)$$

where $\Omega_u$ represents the solid angle of $\mathbf{u}$, and $N$ is the number of electrons in the system. Thus, for any given system, $\langle n_{{\rm XC},\lambda}(u)\rangle$ is a function of one variable, $u$. The relation between this averaged hole and the exchange-correlation energy is immediate, from Eq. 7,

$$E_{{\rm XC},\lambda} = N\int_0^\infty du\; 2\pi u\;\langle n_{{\rm XC},\lambda}(u)\rangle. \qquad (15)$$

Thus any good approximation to $\langle n_{{\rm XC},\lambda}(u)\rangle$ will yield a good approximation to $E_{{\rm XC},\lambda}$.

In Figs. 4 and 5, we plot the system-averaged exchange and correlation holes at full coupling strength in the He atom, taken from our configuration-interaction calculation. We also plot the LSD holes, and the numerical GGA holes (NGGA, defined below) which underlie the construction of PW91. Accurate analytic expressions for the uniform-gas

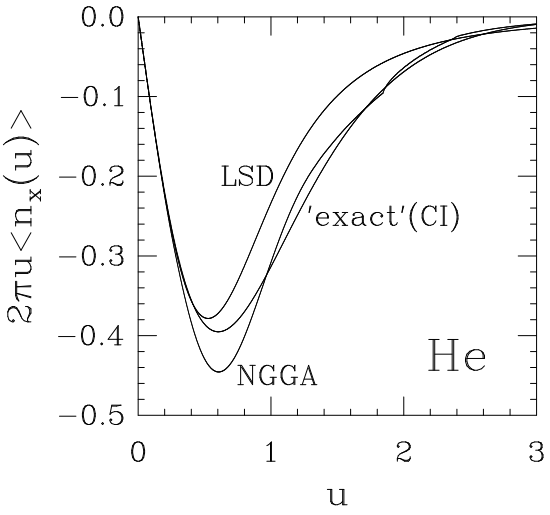


FIG. 4. System-averaged exchange hole density (in atomic units) in the He atom, in LSD, numerical GGA, and exactly (CI). The area under each curve is the exchange energy.

hole are known [44], and were used to construct the LSD hole. We immediately see that LSD is doing a good job of modelling the hole, and GGA does even better.

We can easily understand why LSD does such a good job. The exact system-averaged hole obeys many conditions which have been derived over the years [14,42,45]. Amongst the most important for our purposes [1] are sum rules on the exchange and correlation contributions:

$$\int_0^\infty du\; 4\pi u^2\;\langle n_{\rm X}(u)\rangle = -1, \qquad (16)$$

$$\int_0^\infty du\; 4\pi u^2\;\langle n_{\rm C}(u)\rangle = 0, \qquad (17)$$

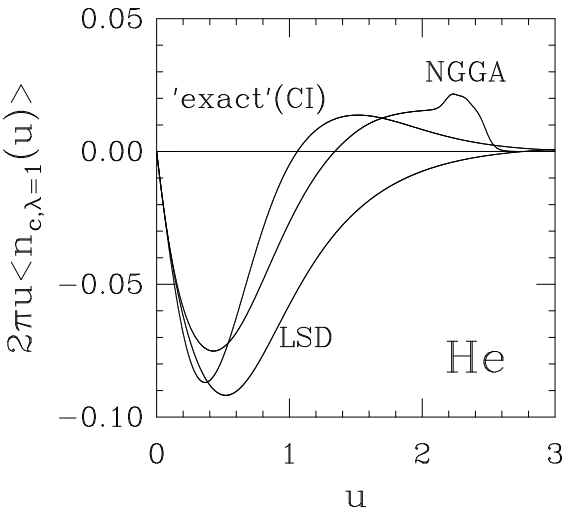


FIG. 5. System-averaged correlation hole density at full coupling strength (in atomic units) in the He atom, in LSD, numerical GGA, and exactly (CI). The area under each curve is the full coupling-strength correlation energy.

the non-positivity of the exchange hole:

$$\langle n_{\rm x}(u)\rangle \le 0, \tag{18}$$

and the cusp condition [46,47] at $u = 0$,

$$\left.\frac{\partial\langle n_{{\rm xc},\lambda}(u)\rangle}{\partial u}\right|_{u=0} = \lambda\big[\langle n_{{\rm xc},\lambda}(0)\rangle + \langle n(0)\rangle\big], \tag{19}$$

where

$$\langle n(u)\rangle = \frac{1}{N}\int\frac{d\Omega_u}{4\pi}\int d^3r\; n(\mathbf{r})\; n(\mathbf{r}+\mathbf{u}). \tag{20}$$

Now, since LSD replaces the exact hole of the inhomogeneous system by that of another physical system, namely the uniform gas, the LSD hole satisfies all these conditions. Furthermore, the on-top exchange hole, $\langle n_{\rm x}(0)\rangle$, is exact in LSD [48–50] (for systems whose exchange wavefunction consists of a single Slater determinant – see section IV below), while the on-top correlation contribution is very accurate [51], although not exact [52]. From the cusp condition, this implies high accuracy for all $u$ close to 0, while the sum rules then constrain LSD from doing too badly as $u$ becomes large. These features can be seen in the plots, and explain why the LSD curves so closely match the exact ones.

To understand the origin of the NGGA curves, consider the construction of PW91 [11,53]. Kohn and Sham [2] already recognized that a simple improvement on LSD might be provided by treating LSD as the zeroth-order term in a Taylor series in the gradients of the density, and therefore including the next higher terms. This defines the gradient expansion approximation (GEA), which includes terms up to $|\nabla n|^2$. Such an expansion works well to improve on the local approximation to the kinetic energy [54]. However, while GEA moderately improves exchange energies, it produces very poor correlation energies. The reason for this failure is clear from our above analysis. In making this extension, we are no longer approximating $\langle n_{\rm xc}(u)\rangle$ by the hole of another physical system, so that the sum rules and non-positivity constraints are violated. Thus the hole is no longer constrained by these conditions, and a poor approximation results.

The real-space cutoff procedure is designed to cure these problems in the gradient expansion [43]. At each point $\mathbf{r}$ in space, all positive portions of the gradient-expanded exchange hole are simply thrown away. Furthermore, beyond a given value of $u$, the rest of the hole is set to zero, with that point chosen to recover the exchange sum rule, Eq. 16. A similar procedure chops off the spurious long-range part of the correlation hole to make it respect Eq. 17. This recipe defines a no-parameter procedure for constructing what we call the numerical generalized gradient approximation to $\langle n_{{\rm xc},\lambda}(u)\rangle$ [17], which in turn yields a numerically-defined semilocal functional which obeys the exact conditions given above. The form of the correlation hole in this procedure was chosen [11] to restore LSD as $u \to 0$, so GGA retains the accuracy of LSD at small $u$. The PW91 functional was constructed to mimic the numerical GGA for moderate values of the gradient, while also incorporating further exact conditions for small and large gradients. The kink at $u \approx 1.8$ in the NGGA exchange hole of Fig. 4 and the bump at $u \approx 2.3$ in the NGGA correlation hole of Fig. 5 are both artifacts of the sharp cut-offs in this procedure [17]. The figures demonstrate that by using the gradient expansion, while still satisfying the exact conditions, the numerical GGA holes are indeed better approximations to the exact ones than LSD, thus demonstrating why PW91 yields better energies than LSD.

### C. On-top exchange-correlation hole

As mentioned above, LSD yields a reasonable description of the exchange-correlation hole, because it satisfies several exact conditions. However, since the correlation hole satisfies a zero sum rule, the scale of the hole must be set by its value at some value of $u$. The local approximation is most accurate at points near the electron. In fact, while not exact at $u = 0$, LSD is highly accurate there. Thus the on-top hole provides the "missing link" between the uniform electron gas and real atoms and molecules [18].

To see this in more detail, consider the ratio of the system-averaged on-top exchange-correlation hole to the system-average of the density itself, $\langle n(0)\rangle$, as defined in Eq. 20. This ratio satisfies the inequalities

$$-1 \le \frac{\langle n_{{\rm xc},\lambda}(0)\rangle}{\langle n(0)\rangle} \le 0, \tag{21}$$

for all systems, both exactly and in LSD. Furthermore, for either fully spin-polarized systems or extremely low density, the on-top pair density vanishes, making this ratio -1, both exactly and in LSD. LSD also becomes exact in the high density $r_s = 0$ or non-interacting $\lambda = 0$ limits, where this ratio equals -1/2 for spin-unpolarized systems, and the approach to this limit is also highly accurate (but not exact). We can see this very clearly in the universal curve plotted in Fig. 6, which is this ratio as a function of the average $r_s$ value in the system, defined for spin-unpolarized systems as

$$\langle r_s \rangle = \frac{\int d^3r \; n^2(\mathbf{r}) \; r_s(\mathbf{r})}{\int d^3r \; n^2(\mathbf{r})}, \tag{22}$$

where

$$r_s(\mathbf{r}) = \left(\frac{3}{4\pi n(\mathbf{r})}\right)^{1/3}. \tag{23}$$

The solid curve was obtained from Yasuhara's expression

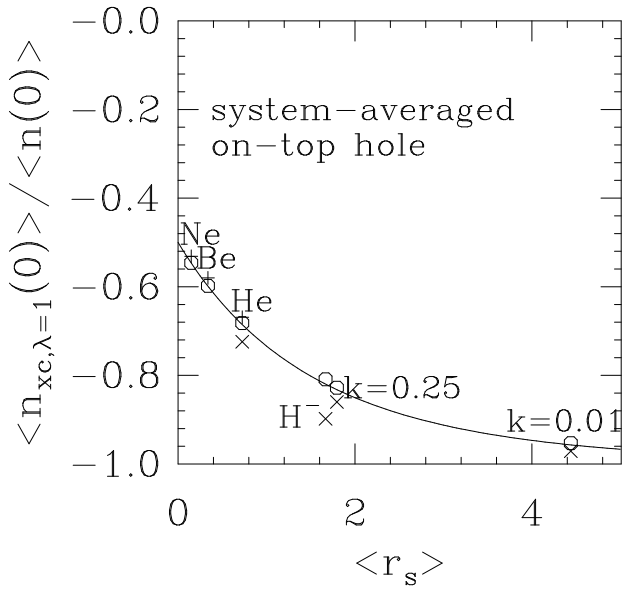


FIG. 6. Universal curve for the system-averaged on-top hole density in spin-unpolarized systems. The solid curve is for the uniform gas. The circles indicate values calculated within LSD, while the crosses indicate essentially exact results, and the plus signs indicate less accurate CI results. The high-density ($r_s \to 0$) and low-density ($r_s \to \infty$) limits behave respectively like the weak-coupling ($\lambda \to 0$) and strong-coupling ($\lambda \to \infty$) limits.

for the on-top hole for a uniform electron gas [55]. The circles indicate the LSD values of $\langle n_{\mathrm{XC},\lambda}(0)\rangle/\langle n(0)\rangle$. Their proximity to the uniform-gas curve indicates that the approximation

$$\langle n^{\mathrm{LSD}}_{\mathrm{XC},\lambda}(0)\rangle \approx n^{\mathrm{unif}}_{\mathrm{XC},\lambda}(\langle r_s\rangle; u = 0) \tag{24}$$

is highly accurate. The crosses represent either almost-exact numerical calculations [36] or exact analytic results for Hooke's atom [56], which consists of two electrons bound to a center by a spring of force constant $k$. The pluses represent CI results, which tend to underestimate the depth of the on-top hole, because of the difficulty in representing the cusp in a finite basis set (see section III D).

The importance of the accuracy of the on-top hole in LSD cannot be over-stressed. This accuracy is not just in the system-average, but is also there on a point-wise basis. In Fig. 7, we plot the ratio of the full-coupling strength on-top exchange-correlation hole to the density as a function of $r$ in the He atom, both exactly, using a very accurate wavefunction [36], and in LSD. We see that already for $r \geq 1$ ($r_s \geq 1.33$), the LSD on-top hole is extremely accurate. Thus, even in the tail region of the density, which is vital to understanding chemistry, the *on-top* LSD hole is highly accurate.

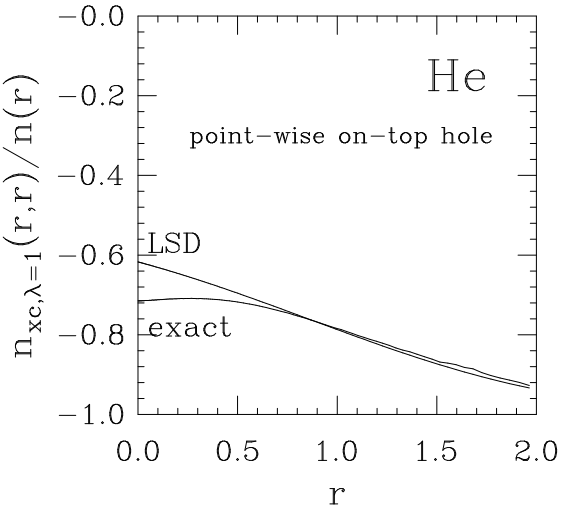


FIG. 7. Local on-top exchange-correlation hole at full coupling strength divided by density as a function of $r$ in the He atom. The nuclear cusp produces greater LSD error for $r \to 0$.

Successful density functional approximations such as the PW91 GGA or the self-interaction correction (SIC) [57] to LSD recover [19] LSD values for the on-top hole density and cusp. The weighted density approximation (WDA) [41,42], which recovers the LSD exchange hole density but not the LSD correlation hole density [19] in the limit $u \to 0$, needs improvement in this respect.

### D. Importance of the uniform gas limit

The accuracy of the on-top hole density has a crucial bearing on the validity of GGA functionals. LSD and GGA are limited-form approximations to $E_{\mathrm{XC},\lambda}$. These limited forms can only be exact for uniform densities. Thus any

GGA ought to be correct, i.e., reduce to LSD, in this limit. Otherwise, it will miss the vital link between the uniform gas and the real system, namely the on-top hole density, as shown in Figs. 6 and 7. Moreover, certain real systems (e.g., close-packed crystals of simple metals) closely resemble a uniform electron gas. However, a very popular GGA in use in quantum chemistry, the Lee-Yang-Parr (LYP) correlation functional [10], does not satisfy this condition. In Table II, we compare the correlation energy in LYP for a uniform gas, as a function of $r_s$, and compare it with the essentially exact value [3,4,57], using the parametrization of Perdew and Wang [4]. We see that LYP does badly for the uniform gas, and therefore does not contain the information about the on-top hole found in functionals which reproduce this limit, such as PW91.

TABLE II. Correlation energy of the uniform electron gas, comparing the highly-accurate parametrization of Perdew and Wang [4] with the LYP functional [10].

| $r_s$ | LYP | accurate | error(%) |
|---|---|---|---|
| 0.01 | -.0674 | -.1902 | -65 |
| 0.05 | -.0656 | -.1413 | -54 |
| 0.1 | -.0635 | -.1209 | -47 |
| 0.5 | -.0502 | -.0766 | -34 |
| 1.0 | -.0394 | -.0598 | -34 |
| 2.0 | -.0270 | -.0448 | -40 |
| 5.0 | -.0135 | -.0282 | -52 |
| 10.0 | -.0075 | -.0186 | -60 |

For the spin-unpolarized uniform electron gas, the LYP correlation energy functional reduces to that of Colle and Salvetti [58], on which LYP is based. McWeeny's work [59] may have contributed to the widespread misimpression that the Colle-Salvetti functional is accurate in this limit. Note however that McWeeny tested Eq. 9 of Ref. [58], and not the further-approximated Eq. 19 of Ref. [58], which is the basis of LYP and other Colle-Salvetti applications, and which is shown in Table II.

A second observation about the LYP functional is that it predicts *no* correlation energy for a fully spin-polarized system of electrons. Yet, in the uniform-density limit, the correlation energy at full spin-polarization is about half that of the unpolarized system [3,4,57]. Even in the Ne atom, the parallel-spin contribution accounts for about 24% of the total correlation energy (section III D).

A recent and much-discussed system with delocalized electrons illustrates the importance of a GGA recapturing the uniform and slowly-varying density limits. Three basic structures have been proposed for the ground state of $C_{20}$: a ring, a bowl, and a cage. Recent accurate calculations using diffusion Monte Carlo [60] place the bowl as the lowest energy structure. These structures differ only very slightly in their correlation energies per carbon atom, and so provide a very sensitive test of approximate treatments. Hartree-Fock calculations make the cage the highest energy and the ring the lowest, while LSD reverses this ordering. Various GGA functional forms, including BLYP, were tested, but only PW91, which does satisfy the slowly-varying constraint, yields the correct energy ordering, at a level of accuracy comparable to variational Monte Carlo. Note that the claim by the authors of Ref. [60], that no GGA works because several GGA forms yielded different answers, is overdrawn.

### E. Long-range asymptotics of the hole

We have recently discovered [19] a new exact formula for the asymptotic behavior of the wavefunction of an atom or molecule, when one coordinate becomes large, namely

$$\lim_{r\to\infty} \Psi_\lambda(\mathbf{r},\sigma,\mathbf{r}_2,\sigma_2,\ldots,\mathbf{r}_N,\sigma_N) = \sqrt{n_\sigma(\mathbf{r})/N}\,\Psi_\lambda^{(+)}(\mathbf{r}_2,\sigma_2,\ldots,\mathbf{r}_N,\sigma_N)\{\hat{\mathbf{r}},\sigma\}. \quad (25)$$

Here $\Psi_\lambda^{(+)}$ is (typically [19]) a ground-state wavefunction of the positive ion (assuming the $N$-electron system is neutral) which remains when one electron has been removed, and the notation $\{\hat{\mathbf{r}},\sigma\}$ indicates a parametric dependence on the coordinates of the departing electron. If the remaining ion is non-degenerate, e.g., for He, then $\Psi_\lambda^{(+)}$ becomes independent of $\hat{\mathbf{r}}$ as $r\to\infty$. However, in the common case when the ion is degenerate, e.g., for Ne, Ar, Kr, Xe, which have non-spherical ions, the ionic wavefunction appearing in Eq. 25 is oriented relative to the direction of the departing electron, no matter how far from the nucleus that electron is.

This long-range correlation effect shows up in both the first-order density matrix and the exchange-correlation hole for finite systems [19]. We concentrate here on the exchange-correlation hole. The general asymptotic form of the pair density is then

$$\lim_{r\to\infty} P_\lambda(\mathbf{r},\mathbf{r}') = n_\lambda^{(+)}(\mathbf{r}')\{\hat{\mathbf{r}}\}\; n(\mathbf{r}), \quad (26)$$

where

$$n_\lambda^{(+)}(\mathbf{r}')\{\hat{\mathbf{r}}\} = (N-1)\sum_{\sigma_1,\ldots,\sigma_{N-1}}\int d^3r_2\;\ldots\int d^3r_{N-1} \times \left|\Psi_\lambda^{(+)}(\mathbf{r}',\sigma',\mathbf{r}_2,\sigma_2,\ldots,\mathbf{r}_{N-1},\sigma_{N-1})\{\hat{\mathbf{r}},\sigma\}\right|^2, \quad (27)$$

i.e., it is the density of the ion with coupling strength $\lambda$, oriented along the direction $\hat{\mathbf{r}}$. (Note that in the case of a non-degenerate ion, there is no orientation dependence.) Eq. 26 implies that the pair correlation function, $g_\lambda(\mathbf{r},\mathbf{r}') = P_\lambda(\mathbf{r},\mathbf{r}')/n(\mathbf{r})n(\mathbf{r}')$, does *not* typically tend to unity in the limit of large separations, contrary to intuitive expectations [1]. Only for $N\to\infty$, i.e., a solid, will $n_\lambda^{(+)}(\mathbf{r}')\{\hat{\mathbf{r}}\}\to n(\mathbf{r}')$, the uncorrelated case. In terms of the exchange-correlation hole density, we find

$$\lim_{r\to\infty} n_{\mathrm{XC},\lambda}(\mathbf{r},\mathbf{r}') = n_\lambda^{(+)}(\mathbf{r}')\{\hat{\mathbf{r}}\} - n(\mathbf{r}'), \qquad (28)$$

i.e., the hole remaining behind an electron at large distances is determined by the $\lambda$-dependent density of the degenerate ion, oriented relative to the departing electron.

We may also decompose the exchange and correlation contributions to this hole. At $\lambda = 0$, the ion density is that of the Kohn-Sham potential with $N-1$ electrons, so Eq. 28 becomes

$$\lim_{r\to\infty} n_x(\mathbf{r},\mathbf{r}') = -|\phi_{\mathrm{HO}}^{\mathrm{KS}}(\mathbf{r}')\{\mathbf{r}\}|^2, \qquad (29)$$

where $\phi_{\mathrm{HO}}^{\mathrm{KS}}$ is the highest-occupied Kohn-Sham orbital, oriented in the general direction $\hat{\mathbf{r}}$. Thus the contribution of exchange to the exchange-correlation hole in the asymptotic limit $r \to \infty$ will typically be some finite fraction which varies with $\mathbf{r}'$.

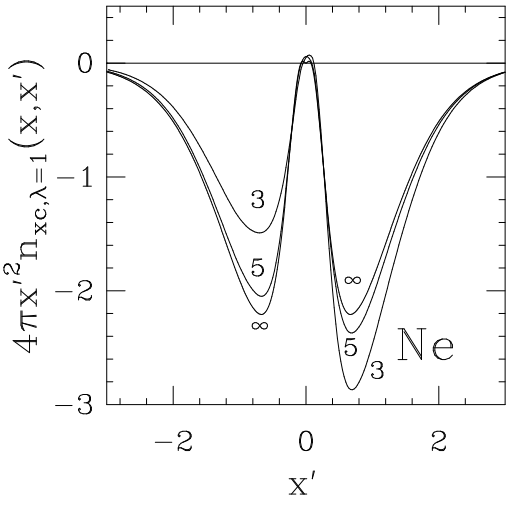


FIG. 8. Full coupling-strength radial exchange-correlation hole density around an electron at $x = 3, 5, \infty$, plotted along the direction of the departing electron.

In the case where the degeneracy is due to symmetry, symmetry arguments may be used to determine $n_\lambda^{(+)}(\mathbf{r}')\{\hat{\mathbf{r}}\}$. For example, the Ne ion has an electron missing in a $2p$ orbital. For the ion density appearing in Eq. 28, the $2p$ hole points in the direction of the distant electron [19]. To illustrate these effects, we plot the radial exchange-correlation hole density $4\pi r'^2 n_{\mathrm{XC},\lambda=1}(\mathbf{r},\mathbf{r}')$ in the Ne atom, for several large values of $r$, for $\mathbf{r} \parallel \mathbf{r}'$, and $\mathbf{r} \perp \mathbf{r}'$. In Fig. 8, we look along the direction of departure of the electron. The hole for $r \to \infty$ has the shape of the radial density of a $p$ orbital, oriented along the plot axis. For finite values of $r$, we observe a deformation of the hole, since the remaining electron in the $p$ orbital moves away from the electron at position $\mathbf{r}$ to the other side of the atom. This deformation occurs even in the exchange (i.e., $\lambda = 0$) hole.

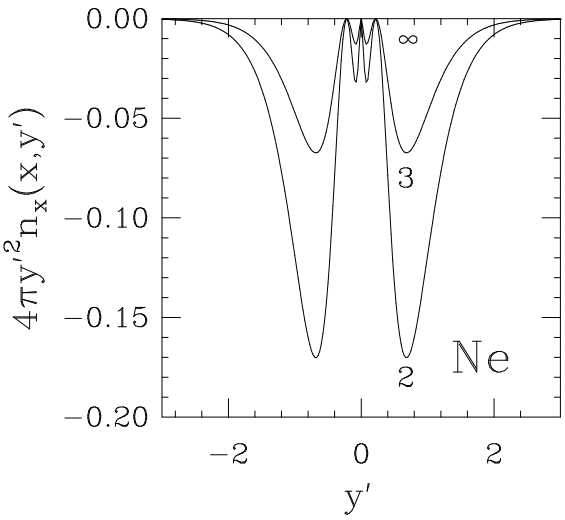


FIG. 9. Hartree-Fock radial hole density around an electron at $x = 2, 3, \infty$, plotted perpendicular to the direction of the departing electron.

For any finite value of $r$, there is a finite probability that the electron at $r$ is either a 1s or a 2s electron, instead of a 2p electron, so that the exchange hole is a hybrid between a hole in an s-shell and a hole in a p-shell [61]. In Fig. 9, we plot the Hartree-Fock hole perpendicular to the direction of departure, for several values of the electron position. The $p$-orbital hole in the ion density vanishes for all

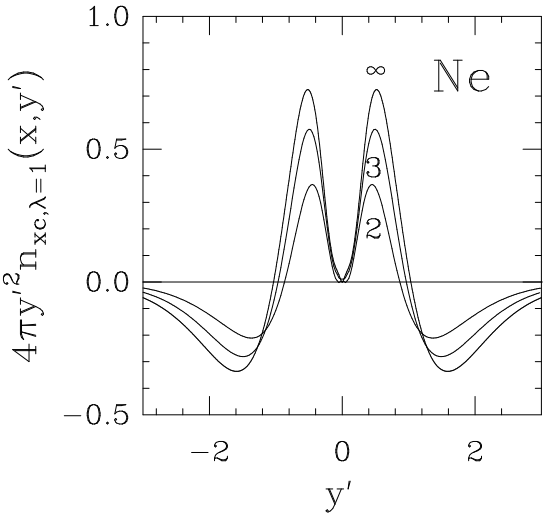


FIG. 10. Full coupling-strength radial exchange-correlation hole density around an electron at $x = 2, 3, \infty$, plotted perpendicular to the direction of the departing electron.

$x'$, so, from Eq. 29, the exchange hole also vanishes for all $x'$ as $r \to \infty$. However, correlation causes the ion density to relax as the electron leaves, and the density moves in toward the nucleus, becoming more compact, to partially fill the hole left behind. This effect is greatest when the electron is furthest, i.e., as $r \to \infty$. In Fig. 10, we plot the full coupling-strength exchange-correlation hole perpendicular to the direction of departure, for the same values of the electron position. Comparison with Fig. 9 shows that correlation dominates the shape of this hole.

In the limit $r \to \infty$, the LSD hole incorrectly spreads out over all space, while the SIC and WDA holes behave [19] exactly or approximately like Eq. 29. The LSD system-averaged hole decays as the uniform-gas hole decays: both exchange and correlation decay as $u^{-4}$, but these long tails cancel in their sum, to yield an exchange-correlation hole which vanishes as $u^{-5}$. This power law decay is quite incorrect in a finite system, when compared with the exponential decay of the hole due to that of $n(\mathbf{r})$. However, the cancellation of exchange and correlation reduces the error due to this tail, and so accounts, to some extent, for the cancellation of errors between the LSD exchange and correlation energies. The GGA behavior, on the other hand, provides an exponential decay for large values of $u$, because of the real-space cut-offs [17].

### F. Relevance of the exchange-correlation potential

In this subsection, we make a simple and direct connection between point-wise quantities and system-averaged quantities. In section II A, we noted several papers which detail the idiosyncrasies of the approximate exchange-correlation potentials, and their considerable deviation from the exact potential. We then showed in section II B how system-averaged quantities were much better approximated by the density functionals. This then raises the question: can we relate the potentials to some more physically meaningful system-averaged quantities, to see how significant the LSD and PW91 errors in the potentials are?

The answer is yes, in a very general way, as has been discussed before [62,63]. Consider any parameter in the external potential, called $\gamma$. For definiteness, we choose the internuclear separation in a diatomic molecule. Then the exchange-correlation energy depends parametrically on this quantity. Now imagine making an infinitesimal change in $\gamma$. The differential change in $E_{\rm XC}$ is

$$\frac{dE_{\rm XC}}{d\gamma} = \int d^3r \; v_{\rm XC}(\mathbf{r}) \; \frac{dn(\mathbf{r})}{d\gamma}, \tag{30}$$

i.e., this change is determined by a system-average of the exchange-correlation potential. Thus one may relate system-averages of the potential to differential changes in the energy. Note that, since the particle number does not change with $\gamma$, there are no difficulties associated with derivative discontinuities. In the specific case we have chosen, the quantity $dE_{\rm XC}/d\gamma$ has direct physical significance, as it goes into the equation determining the equilibrium bond length. Note that, within a fully self-consistent calculation, the equilibrium value of the bond length can be determined directly from the density and external potential alone, but that approximate functionals are usually tested on the exact density, to determine their accuracy. Thus calculations of such quantities might prove very useful in studying the efficacy of functionals.

We have applied a slight variation of this general idea to the exchange-correlation potential of the He atom [18]. The virial theorem applied to the Kohn-Sham system yields [39]:

$$E_{\rm X} = -\int d^3r \; n(\mathbf{r}) \; \mathbf{r} \cdot \nabla v_{\rm X}(\mathbf{r}) \tag{31}$$

and

$$E_{\rm C} + T_{\rm C} = -\int d^3r \; n(\mathbf{r}) \; \mathbf{r} \cdot \nabla v_{\rm C}(\mathbf{r}). \tag{32}$$

Thus, just as in the case of the energy densities, the small- and large-$r$ behaviors of the potential receive very little weight in the energy integrals, leading to the dramatic results of row 6 of Table I. These results indicate that the potential in PW91 is far better than that of LSD in terms of energies (and is also the right way up).

## III. UNDERSTANDING NONLOCALITY

In this section, we examine the concept of nonlocality, in the sense of how much error LSD makes. We have seen in the previous section that LSD is most accurate near $u = 0$, and least accurate at large $u$. Thus the deeper the hole is at the origin, and therefore, from the sum rule, the shorter its range in $u$, the better approximated it should be in LSD.

### A. Coupling-constant decomposition

We tested this idea [18] by examining the holes and corresponding energies of three different coupling constants: $\lambda = 0$ (exchange), $\lambda = 1$ (full coupling strength), and averaged over $\lambda$ (as in the actual $E_{\rm XC}$)). Since the on-top correlation hole is negative, the shallowest of these holes is the exchange hole, followed by the coupling-constant averaged hole, and the deepest is the full coupling-strength hole. This behavior is illustrated for the uniform electron gas in Fig. 6 of Ref. [18], and these qualitative features should be shared by the system-averaged holes of most inhomogeneous systems. This is borne out by the results of Table 2 of Ref. [18], in which the error in LSD atomic energies, measured relative to their PW91 counterparts, was tabulated for the energies of the three different holes. This error

is largest for exchange and least for full coupling strength, and this effect becomes less significant as we approach the high-density limit. This is consistent with our idea that the deeper the on-top hole is, the more local is the corresponding energy.

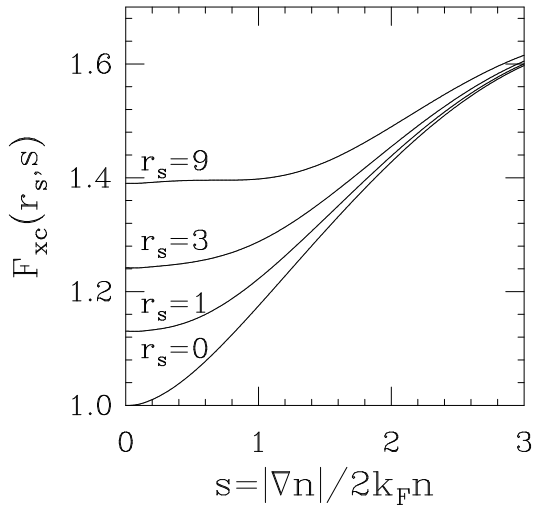


FIG. 11. Enhancement factor over local exchange, $F_{\rm XC}(r_s,s)$, for spin-unpolarized systems in the PW91 GGA.

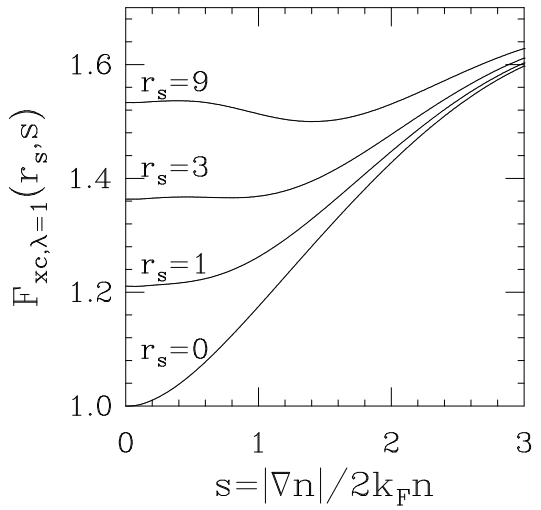


FIG. 12. Full coupling-strength enhancement factor over local exchange, $F_{{\rm XC},\lambda=1}(r_s,s)$, for spin-unpolarized systems in the PW91 GGA.

An alternative way to see this effect is to consider the enhancement factor over local exchange in PW91. We may write any GGA energy, for spin-unpolarized systems, as

$$E_{{\rm XC},\lambda}^{\rm GGA} = \int d^3r\ n(\mathbf{r})\ \epsilon_{\rm X}(r_s)\ F_{{\rm XC},\lambda}(r_s,s), \tag{33}$$

where

$$s = |\nabla n|/2k_F n, \tag{34}$$

, $k_F = (3\pi^2 n)^{1/3}$ is the Fermi wavevector, and

$$F_{{\rm XC},\lambda}(r_s,s) = \left(1 + r_s \frac{\partial}{\partial r_s}\right) F_{\rm XC}(\lambda r_s, s), \tag{35}$$

where the differentiation with respect to $r_s$ undoes the coupling-constant integral implicit in $F_{\rm XC}(r_s,s)$. Eq. 35 at $\lambda = 1$ was found in Ref. [64], and used to calculate $T_{\rm C}$ in Ref. [65]. Then the enhancement factors for exchange, exchange-correlation, and exchange-correlation at full coupling strength are $F_{\rm X}(s) = F_{{\rm XC},\lambda=0}(r_s,s) = F_{{\rm XC},\lambda}(r_s = 0,s)$, $F_{\rm XC}(r_s,s) = \int_0^1 d\lambda\ F_{{\rm XC},\lambda}(r_s,s)$, and $F_{{\rm XC},\lambda=1}(r_s,s)$, respectively. In Figures 11 and 12 we plot $F_{\rm XC}(r_s,s)$ and $F_{{\rm XC},\lambda=1}(r_s,s)$ for PW91. At the LSD level, we would have $F_{{\rm XC},\lambda}(r_s,s) = F_{{\rm XC},\lambda}(r_s,s=0)$, i.e., horizontal lines. Since the full coupling-strength curves change far less as a function of $s$, the full coupling-strength functional of Fig. 12 is more local than its coupling-constant averaged counterpart of Fig. 11. Furthermore, the greatest nonlocality occurs at $r_s = 0$, which is the exchange curve. These results further confirm our intuitive idea that the degree of nonlocality is strongly related to the spatial extent of the hole.

### B. Hybrid functionals

Following the "B3" proposal of Becke [30], several schemes for mixing Hartree-Fock into density functional treatments have appeared in the literature [30,31]. To get the correct energy for the slowly-varying electron gas, this hybrid functional must simplify to [18]

$$E_{\rm XC} \approx (1-a)E_{\rm X}^{\rm GGA} + aE_{\rm X}^{\rm HF} + E_{\rm C}^{\rm GGA}. \tag{36}$$

This "B1" form has recently been proposed independently by Becke [66], to reduce the number of empirical parameters in the original "B3" form.

To determine how much HF is needed, we consider systems where $s$ is significantly greater than 1, but where GGA still works reasonably well. In Ref. [18], we examined the ionization potentials, electron affinities, and electronegativities of a variety of atoms, as well as the atomization energies of several closed-shell hydrocarbon molecules. By examining root-mean-square errors in the energies, we found results consistent with those of Becke [30], namely that $a \approx 0.2$ slightly improved the PW91 results. However, in Table III, we list a variety of root-mean-square energy errors $\Delta_a$ for some other systems, for several values of the mixing parameter $a$: $a = 0$ corresponds to no mixing (PW91), $a = 0.2$ corresponds to the amount of mixing recommended by Becke (B1), $a = 1$ corresponds to Hartree-Fock exchange and

TABLE III. Various properties evaluated using the hybrid functional of Eq. 36. We report root-mean-square errors in energies $\Delta_a$ (in eV) as a function of the mixing parameter $a$, and the optimum value of $a$. The properties and data sets on which they are evaluated are described in the text. All results were extracted from Tables V and VII of Ref. [13]. (1 eV = 23.06 kcal/mole.)

| energy | $\Delta_0$ | $\Delta_{0.2}$ | $\Delta_1$ | $\Delta_{\min}$ | $a_{\min}$ |
|---|---|---|---|---|---|
| $\chi$ (term-conserving) | 0.08 | 0.11 | 0.51 | 0.07 | 0.03 |
| $E_{\rm atom}$ (open-shell) | 0.19 | 0.66 | 4.08 | 0.02 | 0.04 |

PW91 correlation, while $\Delta_{\min}$ is the minimum root-mean-square error, achieved at $a = a_{\min}$. The first row reports the electronegativity errors calculated over a subset of atoms, namely those in which the ground-state term of the negative ion is the same as that of the positive ion [13], the two ionic configurations differing by $(ns)^2$. Now $a = 0$ is clearly better than $a = 0.2$, and only marginally worse than the optimum value $a = 0.03$. These results are consistent with the suggestion that local (and semilocal) approximations to ionization potentials and electron affinities suffer from interterm and interconfigurational errors in their treatment of exchange [1]. These 12 term-conserving $s$-process electronegativities should not suffer from this error, and indeed need far less mixing with Hartree-Fock. However, this row also shows that $a = 0.2$ is not optimal for these processes.

The last row of Table III lists the error in the atomization energy of a single hydrocarbon molecule, $C_2$. This molecule is "abnormal", in the sense that no single determinant dominates its wavefunction [67]. It has low-lying excited states close to its ground-state. The HF atomization energy is seriously in error [13]. Hence the $a = 0.2$ error is far greater than the PW91 ($a = 0$) error.

Although the adiabatic connection formula of Eq. 8 justifies a certain amount of Hartree-Fock mixing, there are situations in which $a$ should vanish. In a spin-restricted description of the molecule $H_2$ at large bond length (section IV) the Hartree-Fock or $\lambda = 0$ hole is equally distributed over both atoms, and is independent of the electron's position. But the hole for any finite $\lambda$, however small, is entirely localized on the electron's atom, so no amount of Hartree-Fock mixing is acceptable in this case.

Thus we have argued that the only hybrid form which is correct for the slowly-varying densities is that of Eq. 36, with a value of $a$ between 0 and 0.2. Note that the approximation $a = 1$, which reproduces exact exchange, ignores the cancellation of nonlocalities between the exchange and correlation energies, and the fourth column of Table III shows how poor the latter approximation is.

As discussed in the previous sections, LSD works well, and GGA does better, by modelling the system-averaged hole in a way which respects the sum rules, amongst other things. A much better way to construct a hybrid functional [54,68] would be to construct a hybrid hole, in which the small-separation contributions would be modelled in LSD (or GGA), which works well here, and the large-separation contributions would be modelled by some approximation designed to work at large distances, e.g., the random phase approximation [35], or the correct asymptotic limit [19].

### C. Spin decomposition

Another way to separate short- and long-range effects is via the spin decomposition. We may decompose Eq. 4 by writing

$$P_\lambda(\mathbf{r}\sigma,\mathbf{r}'\sigma') = N(N-1)\sum_{\sigma_3,\ldots,\sigma_N}\int d^3r_3\ \ldots\int d^3r_N \times\left|\Psi_\lambda(\mathbf{r},\sigma,\mathbf{r}',\sigma',\ldots,\mathbf{r}_N,\sigma_N)\right|^2, \qquad (37)$$

where $\sigma = \uparrow$ or $\downarrow$, which in turn leads to a spin-decomposed hole:

$$P_\lambda(\mathbf{r}\sigma,\mathbf{r}'\sigma') = n_\sigma(\mathbf{r})\ \left(n_{\sigma'}(\mathbf{r}') + n_{{\rm XC},\lambda}(\mathbf{r}\sigma,\mathbf{r}'\sigma')\right), \qquad (38)$$

where $n_\sigma(\mathbf{r})$ is the density of spin $\sigma$, and to a spin-decomposed energy:

$$E^{\sigma,\sigma}_{{\rm XC},\lambda} = \frac{1}{2}\int d^3r\ \int d^3r'\ \frac{P_\lambda(\mathbf{r}\sigma,\mathbf{r}'\sigma) - n_\sigma(\mathbf{r})n_\sigma(\mathbf{r}')}{|\mathbf{r}-\mathbf{r}'|},$$
$$E^{\uparrow\downarrow}_{{\rm XC},\lambda} = \int d^3r\ \int d^3r'\ \frac{P_\lambda(\mathbf{r}\uparrow,\mathbf{r}'\downarrow) - n_\uparrow(\mathbf{r})n_\downarrow(\mathbf{r}')}{|\mathbf{r}-\mathbf{r}'|}. \qquad (39)$$

Note that both antiparallel holes ($\uparrow\downarrow$ and $\downarrow\uparrow$) give the same contribution to the energy, and are conventionally added together into one antiparallel contribution, $E^{\uparrow\downarrow}_{{\rm XC},\lambda}$ as defined here.

We focus on the correlation energy only, as all the exchange energy is in the parallel-spin channels. Before we consider the question of locality of the different spin contributions, we first note that, contrary to assumptions in the literature [69,70], while the antiparallel contribution is typically most of the correlation energy, the parallel contribution is often not negligible. For spin-unpolarized systems, if $N = 2$, *all* the correlation is antiparallel, while for $N \to \infty$ in the uniform gas, only 60% is antiparallel. As far as we know, all other spin-unpolarized systems fall between these two extremes. As we report below, for Ne, a full 24% of the correlation energy is in the parallel-spin channels.

We now consider the locality of the antiparallel-spin contribution to the correlation energy, relative to the total correlation energy. The holes corresponding to both these contributions obey the zero sum rule, Eq. 17. However, the parallel-spin on-top correlation hole vanishes, suggesting that this hole will extend further out from the electron's position, and therefore be less well-approximated by LSD. In Table IV we compare the full correlation energy with just the antiparallel-spin contribution. We used the approximate

TABLE IV. Errors in LSD correlation energies, relative to PW91, for several atoms (%). The results were calculated from the entries in Table III of Ref. [35].

| Atom | $\Delta E_C$ | $\Delta E_C^{\uparrow\downarrow}$ |
|---|---|---|
| H | 236 | 0 |
| He | 145 | 58 |
| Li | 162 | 60 |
| N | 114 | 37 |
| Ne | 94 | 42 |
| Ar | 85 | 37 |
| Kr | 71 | 32 |
| Xe | 64 | 30 |

GGA for antiparallel spin described in Ref. [35], which predicts that 20% of the correlation energy of Ne is from antiparallel spin. Clearly, the antiparallel contribution is much more local than the total.

### D. Hybrid density functional-wavefunction methods

The results of the previous section suggest that a good hybrid method might treat antiparallel spin using a GGA, while using a wavefunction treatment for parallel-spin [54]. Since the parallel-spin hole has no cusp and is of greater spatial extent, this contribution should be more accesible to a wavefunction method beginning from one-particle wave functions, such as CI.

To test this idea, we performed a Moller-Plesset (MP2) [71] perturbation calculation for the Ne atom, in which we spin-decomposed the correlation energy. The details of the calculation are given in Appendix B. These results are very close to values which may be extracted from Ref. [72], which we discovered after completing this work. We chose Ne because it is well known that MP2 gives an accurate account of the correlation energy of this atom. The parallel- and antiparallel-spin contribution to the MP2 correlation energy ($E_2$) for a number of different gaussian basis sets are given in Table V. As expected, the MP2 correlation energy is very close in almost all cases to the correlation energy obtained from multireference configuration-interaction (CI) calculations. We assume that the MP2 spin-decomposed correlation contributions are as close to the spin-decomposed correlation energies of the elaborated CI calculations as the total correlation energies are. Comparison of the parallel- and antiparallel-spin correlation contributions obtained with the 14s9p4d3f1g basis set (which gives a CI correlation energy close to the exact value of -0.3917 (hartree) [73]) shows that the parallel-spin contribution is a significant fraction (24%) of the total correlation energy.

TABLE V. Gaussian basis sets and corresponding spin-decomposed correlation energies (in hartree) for the Ne atom.

| Basis set | $E_c^{CI}$ | $E_2$ | $E^{\uparrow\uparrow}+E^{\downarrow\downarrow}$ | $E^{\uparrow\downarrow}$ | $\frac{E_2^{\uparrow\uparrow}+E_2^{\downarrow\downarrow}}{E_2}$ |
|---|---|---|---|---|---|
| $4s2p$ | -0.12204 | -0.12390 | -0.03127 | -0.09263 | 0.25 |
| $3s2p1d$ | -0.14852 | -0.14892 | -0.04231 | -0.10661 | 0.28 |
| $5s3p1d$ | -0.22420 | -0.22795 | -0.05998 | -0.16797 | 0.26 |
| $14s9p4d3f$ | -0.34936 | -0.34556 | -0.08297 | -0.26258 | 0.24 |
| $14s9p4d3f1g$ | -0.35822 | -0.35476 | -0.08365 | -0.27111 | 0.24 |

From the last column of the table, we see that the ratio of the parallel-spin to the total correlation energy is remarkably independent of the size of the basis set. Contrary to expectation, the parallel-spin correlation contribution appears to be about as difficult to account for within a finite basis-set approach as the antiparallel-spin correlation. Our investigation does not provide a careful study of the basis-set saturation behavior in MP2 calculations, such as given in Refs. [74,72,75,33]. However, our results show that, with small- and moderate-sized basis sets which are sufficiently flexible for most purposes and computationaly tractable in calculations on larger systems, there is no evidence that the parallel-spin correlation contribution converges more rapidly than the antiparallel-spin contribution. A plausible explanation for this effect is that, for small interelectronic separations, the wavefunction becomes a function of the separation, which is difficult to represent in a finite basis-set approach for either spin channel. The cusp condition of Eq. 19 is a noticeable manifestation of this dependence, but does not imply that the antiparallel-spin channel is more difficult to describe with a moderate-sized basis set than the parallel channel. In fact, in the parallel correlation hole, there is a higher-order cusp condition, relating the second and third derivatives with respect to $u$ [76].

It is also clear from Table V that the *absolute* basis-set truncation error in Ne is about three times bigger for the antiparallel-spin correlation energy than for parallel. Thus the proposed spin-analysis hybrid of Ref. [35] may yet have some (limited) utility.

## IV. ABNORMAL SYSTEMS AND EXTREME NONLOCALITY

We define a "normal" system as one in which the hole density at the weakly-interacting end of the coupling-constant integration is close to that of a single Slater determinant. In such a system, the local and gradient-corrected holes, evaluated for the exact spin-densities, are nearly exact near the position of the electron they surround. As a result, the exchange-correlation energy is approximately a local functional of the exact spin densities. In this section, we show that accurate on-top hole densities in "abnormal" systems like stretched $H_2$ are found for a quite different reason: the self-consistent spin magnetization density goes wrong, in order to make the on-top hole density (and the associated energy) right [36].

At the equilibrium bond length of $H_2$, the LSD or GGA equations have a single self-consistent ground-state solution

with $m(\mathbf{r}) = 0$. But, at a larger internuclear separation, this solution bifurcates and a second solution of "broken symmetry" and lower energy appears. In the limit of infinite separation, this second solution describes one hydrogen atom with an electron of spin up on the left, and another with an electron of spin down on the right. The molecular dissociation energies calculated for these two solutions pose a dilemma: The LSD or GGA energy is nearly exact for the broken-symmetry solution with qualitatively incorrect spin densities, and seriously in error if the correct physical spin symmetry (singlet [77]) is imposed on the spin densities, as shown in Table 1 of Ref. [36]. (This symmetry- breaking also occurs in Hartree-Fock theory.)

Evidently, the LSD and GGA approximations are working, but not in the way the standard spin-density functional theory would lead us to expect. In Ref. [36], a nearly-exact alternative theory, to which LSD and GGA are also approximations, is constructed, which yields an alternative physical interpretation in the absence of a strong external magnetic field. In this theory, $n_\uparrow(\mathbf{r})$ and $n_\downarrow(\mathbf{r})$ are not the physical spin densities, but are only intermediate objects (like the Kohn-Sham orbitals or Fermi surface) used to construct two physical predictions: the total electron density $n(\mathbf{r})$ from

$$\tilde{n}(\mathbf{r}) = n_\uparrow(\mathbf{r}) + n_\downarrow(\mathbf{r}), \tag{40}$$

and the full-coupling strength on-top electron pair density $P_{\lambda=1}(\mathbf{r},\mathbf{r})$ from its LSD or GGA approximation

$$\tilde{P}_{\lambda=1}(\mathbf{r},\mathbf{r}) = P^{\rm unif}_{\lambda=1}(n_\uparrow(\mathbf{r}), n_\downarrow(\mathbf{r}); u=0), \tag{41}$$

where $P^{\rm unif}_{\lambda=1}(n_\uparrow, n_\downarrow; u=0)$ is the full coupling-strength on-top pair density for an electron gas with uniform spin densities $n_\uparrow$ and $n_\downarrow$.

Since (for fixed $n_\uparrow + n_\downarrow$) $P^{\rm unif}_{\lambda=1}(n_\uparrow, n_\downarrow; u=0)$ is an *even* function of $n_\uparrow - n_\downarrow$, this alternative interpretation encounters no LSD or GGA spin-symmetry dilemma. In the separated-atom limit for $H_2$, it correctly makes $P_{\lambda=1}(\mathbf{r},\mathbf{r}) = 0$ for $\mathbf{r}$ in the vicinity of either atom, since (by the Pauli exclusion principle) $P^{\rm unif}_{\lambda=1}(n_\uparrow, n_\downarrow; u=0)$ vanishes when either $n_\uparrow$ or $n_\downarrow$ vanishes.

The two physical interpretations of LSD and GGA are about equally plausible in a "normal" system. But, especially in "abnormal" systems, these approximations may be more faithful to the alternative theory, because of the close relationship between $P_{\lambda=1}(\mathbf{r},\mathbf{r})$ and the electron-electron potential energy of Eq. 5. Thus, accurate total energies are expected to accompany accurate on-top pair densities. Indeed, the new interpretation helps to explain why LSD and GGA yield accurate total energies, and why in practice spin-density functional calculations of the energy are more accurate than total-density ones even in the absence of an external magnetic field, where *formally* $n(\mathbf{r})$ by itself suffices. Of course, when there is a strong external magnetic field coupled to the physical spin magnetization density $m(\mathbf{r})$, the alternative interpretation (which makes no prediction for $m(\mathbf{r})$) is inappropriate.


## ACKNOWLEDGMENTS

This work has been supported by NSF grant DMR95-21353 and by the Deutsche Forschungsgemeinschaft. We thank Andreas Savin for supplying us with accurate values of the local on-top hole density in the He atom.


## APPENDIX A: DETAILS OF CONFIGURATION INTERACTION (CI) CALCULATIONS.

The wave functions for the Ne and Be atoms which we used in this work are described in detail in Ref. [19].

The CI wave function for the He atom was calculated with the COLUMBUS program system [78,79], which contains a program for the generation of the one- and two-particle density matrix of multireference single- and double-excited CI wave functions [79]. The gaussian basis set used for this calculation was an uncontracted $9s4p3d$ basis, as contained in the MOLCAS basis set library [80]. The correlation energy obtained with this basis set was -0.04014 Hartree. To generate the data used in Figure 2 the gaussian basis set was further augmented with two f functions with exponents 1.5 and 0.6. The resulting wave function gives a correlation energy of -0.04101 Hartree.

## APPENDIX B: DETAILS OF MP2 CALCULATION OF SPIN-DECOMPOSITION.

The total correlation energy, as obtained from a second-order Moller-Plesset (MP2) [71] calculation, can easily be split into parallel- and antiparallel-spin contributions. The MP2 energy $E_2$ is given by [81]

$$E_2 = \frac{1}{2}\sum_{\tilde{i}\tilde{j}\tilde{a}\tilde{b}} \frac{\langle\tilde{i}\tilde{j}|V|\tilde{a}\tilde{b}\rangle\big(\langle\tilde{i}\tilde{j}|V|\tilde{a}\tilde{b}\rangle - \langle\tilde{i}\tilde{j}|V|\tilde{b}\tilde{a}\rangle\big)}{\epsilon_{\tilde{a}} + \epsilon_{\tilde{b}} - \epsilon_{\tilde{i}} - \epsilon_{\tilde{j}}}, \tag{B1}$$

where $\tilde{i}$ and $\tilde{j}$ are the indices of the spin orbitals which are occupied at the Hartree-Fock level, and $\tilde{a}$ and $\tilde{b}$ are indices of unoccupied spin orbitals. The orbitals $\varphi_{\tilde{i}}$ are obtained from a Hartree-Fock calculation and the $\epsilon_{\tilde{i}}$ denote the orbital energies. The expectation values $\langle\tilde{i}\tilde{j}|V|\tilde{a}\tilde{b}\rangle$ are given by $\langle\tilde{i}\tilde{j}|V|\tilde{a}\tilde{b}\rangle = \int d^3\mathbf{r}_1 d^3\mathbf{r}_2\ \varphi_{\tilde{i}}(\mathbf{r}_1)\varphi_{\tilde{a}}(\mathbf{r}_1)\frac{\langle\sigma_{\tilde{i}}|\sigma_{\tilde{a}}\rangle\langle\sigma_{\tilde{j}}|\sigma_{\tilde{b}}\rangle}{|\mathbf{r}_1-\mathbf{r}_2|}\varphi_{\tilde{j}}(\mathbf{r}_2)\varphi_{\tilde{b}}(\mathbf{r}_2)$. The sum in Eq. B1 will now be decomposed into sums over all possible spin combinations. With this aim in view we split off the spin component $\uparrow$ or $\downarrow$ of the spin orbitals and obtain

$$\sum_{\tilde{i}\tilde{j}\tilde{a}\tilde{b}} = \sum_{a\uparrow b\uparrow i\uparrow j\uparrow} + \sum_{a\downarrow b\downarrow i\downarrow j\downarrow} + \sum_{a\uparrow b\downarrow i\uparrow j\downarrow} + \sum_{a\downarrow b\uparrow i\downarrow j\uparrow} + \sum_{a\uparrow b\downarrow i\downarrow j\uparrow} + \sum_{a\downarrow b\uparrow i\uparrow j\downarrow}. \tag{B2}$$

The first two terms on the right hand side of this equation involve only parallel-spin electrons and therefore give rise to parallel-spin correlation contributions of the form

$$E_2^{\uparrow\uparrow} + E_2^{\downarrow\downarrow} = \sum_{ijab} \frac{\langle ij|V|ab\rangle \left(\langle ij|V|ab\rangle - \langle ij|V|ba\rangle\right)}{\epsilon_a + \epsilon_b - \epsilon_i - \epsilon_j}, \tag{B3}$$

with
$\langle ij|V|ab\rangle = \int d^3\mathbf{r}_1 d^3\mathbf{r}_2 \; \varphi_i(\mathbf{r}_1)\varphi_a(\mathbf{r}_1)\frac{1}{|\mathbf{r}_1-\mathbf{r}_2|}\varphi_j(\mathbf{r}_2)\varphi_b(\mathbf{r}_2)$. The third and fourth terms describe the interaction of electrons with antiparallel spin. The contribution from these terms is given by

$$E_2^{\uparrow\downarrow} = \sum_{ijab} \frac{|\langle ij|V|ab\rangle|^2}{\epsilon_a + \epsilon_b - \epsilon_i - \epsilon_j}. \tag{B4}$$

Note that the exchange integral $\langle i\downarrow j\uparrow|V|b\uparrow a\downarrow\rangle$ vanishes in this case. The last two terms of Eq. B2 show a spin flip of the electrons as they are excited from orbital $i$ to orbital $a$ and from orbital $j$ to orbital $b$. This contribution vanishes, since the Coulomb interaction between the particles does not cause a spin flip.

The contracted 4s2p, 3s2p1d, and 5s3p1d basis sets in Table IV are the double-zeta, double-zeta plus polarization, and triple-zeta plus polarization basis sets from the TURBOMOLE [82] basis-set library. The CI calculations with these gaussian basis-sets were of single-reference single- and double-excited CI type. The multireference CI calculation for the Ne atom with the uncontracted 14s9p4d3f basis is described in Ref. [19]. This calculation was repeated with an additional g function with the exponent 2.88 leading to the results for the 14s9p4d3f1g basis set reported in Table IV.

---


* To be reprinted in *Density Functional Methods in Chemistry*, eds. B.B. Laird, R. Ross, and T. Ziegler, American Chemical Society Symposium Series.

[1] R.O. Jones and O. Gunnarsson, Rev. Mod. Phys. **61**, 689 (1989).

[2] W. Kohn and L.J. Sham, Phys. Rev. **140**, A 1133 (1965).

[3] S. H. Vosko, L. Wilk, and M. Nusair, Can. J. Phys. **58**, 1200 (1980).

[4] J. P. Perdew and Y. Wang, Phys. Rev. B **45**, 13244 (1992).

[5] Peter Fulde, *Electron Correlations in Molecules and Solids* (Springer-Verlag, Berlin, 1991).

[6] D.C. Langreth and M.J. Mehl, Phys. Rev. B **28**, 1809 (1983).

[7] J.P. Perdew, Phys. Rev. B **33**, 8822 (1986); **34**, 7406 (1986) (E).

[8] J.P. Perdew and Y. Wang, Phys. Rev. B **33**, 8800 (1986); **40**, 3399 (1989) (E).

[9] A.D. Becke, Phys. Rev. A **38**, 3098 (1988).

[10] C. Lee, W. Yang, and R.G. Parr, Phys. Rev. B **37**, 785 (1988).

[11] J.P. Perdew, in *Electronic Structure of Solids '91*, edited by P. Ziesche and H. Eschrig (Akademie Verlag, Berlin, 1991).

[12] J. P. Perdew and K. Burke, in *Proceedings of the 8th International Congress of Quantum Chemistry, 19-24 June, 1994, Prague*, to appear in Int. J. Quantum Chem.

[13] J. P. Perdew, J. A. Chevary, S. H. Vosko, K. A. Jackson, M. R. Pederson, D.J. Singh, and C. Fiolhais, Phys. Rev. B **46**, 6671 (1992); **48**, 4978 (1993) (E).

[14] K. Burke, J. P. Perdew, and M. Levy, in *Modern Density Functional Theory: A Tool for Chemistry*, edited by J. M. Seminario and P. Politzer (Elsevier, Amsterdam, 1995).

[15] B. Hammer, K. W. Jacobsen, and J. K. Nørskov, Phys. Rev. Lett. **70**, 3971 (1993).

[16] L. Stixrude, R. E. Cohen, and D. J. Singh, Phys. Rev. B **50**, 6442 (1994).

[17] K. Burke, J.P. Perdew, and M. Ernzerhof, *Accuracy of density functionals and system-averaged exchange-correlation holes*, in preparation for Phys. Rev. Lett.

[18] K. Burke, J.P. Perdew, and M. Ernzerhof, *Why semi-local functionals work: Universality of the on-top hole density*, in preparation for J. Chem. Phys.

[19] M. Ernzerhof, K. Burke, and J.P. Perdew, *Long-range asymptotic behavior of ground-state wavefunctions, one-matrices, and pair densities*, submitted to J. Chem. Phys.

[20] C. J. Umrigar and X. Gonze, in *High Performance Computing and its Application to the Physical Sciences*, Proceedings of the Mardi Gras 1993 Conference, edited by D. A. Browne *et al.* (World Scientific, Singapore, 1993).

[21] C. J. Umrigar and X. Gonze, Phys. Rev. A **50**, 3827 (1994).

[22] C. Filippi, C. J. Umrigar, and M. Taut, J. Chem. Phys. **100**, 1290 (1994).

[23] J.P. Perdew, R.G. Parr, M. Levy, and J.L. Balduz, Jr., Phys. Rev. Lett. **49**, 1691 (1982).

[24] J. P. Perdew, in *Density Functional Methods in Physics*, edited by R.M. Dreizler and J. da Providencia (Plenum, NY, 1985), p. 265.

[25] M.K. Harbola and V. Sahni, Phys. Rev. Lett. **62**, 489 (1989).

[26] V. Sahni and M.K. Harbola, Int. J. Quantum Chem. S **24**, 569 (1990).

[27] Y. Wang, J. P. Perdew, J. A. Chevary, L. D. MacDonald, and S. H. Vosko, Phys. Rev. A **41**, 78 (1990).

[28] A. Holas and N.H. March, Phys. Rev. A **51**, 2040 (1995).

[29] M. Levy and N.H. March, *Path-integral formulas for exchange and correlation potentials separately*, preprint.

[30] A.D. Becke, J. Chem. Phys. **98**, 1372 (1993).

[31] V. Barone, Chem. Phys. Lett. **226**, 392 (1994).

[32] W. Kutzelnigg and W. Klopper, J. Chem. Phys. **94**, 1985 (1991).

[33] V. Termath, W. Klopper, and W. Kutzelnigg, J. Chem. Phys. **94**, 2002 (1991).

[34] W. Klopper and W. Kutzelnigg, J. Chem. Phys. **94**, 2020 (1991).

[35] J.P. Perdew, Int. J. Quantum Chem. S **27**, 93 (1993).

[36] J.P. Perdew, A. Savin, and K. Burke, Phys. Rev. A **51**, 4531 (1995).
[37] R.G. Parr and W. Yang, *Density Functional Theory of Atoms and Molecules* (Oxford, New York, 1989).
[38] D.C. Langreth and J.P. Perdew, Solid State Commun. **17**, 1425 (1975).
[39] M. Levy and J.P. Perdew, Phys. Rev. A **32**, 2010 (1985).
[40] A. Görling and M. Ernzerhof, Phys. Rev. A **51**, 4501 (1995).
[41] O. Gunnarsson and B.I. Lundqvist, Phys. Rev. B **13**, 4274 (1976).
[42] O. Gunnarsson, M. Jonson, and B. I. Lundqvist, Phys. Rev. B **20**, 3136 (1979).
[43] K. Burke and J. P. Perdew, in *Thirty Years of Density Functional Theory, 13-16 June, 1994, Cracow*, to appear in Int. J. Quantum Chem.
[44] J. P. Perdew and Y. Wang, Phys. Rev. B **46**, 12947 (1992).
[45] M. Levy, in *Density Functional Theory*, eds. R. Dreizler and E. K. U. Gross, NATO ASI Series (Plenum, New York, 1995).
[46] J. C. Kimball, Phys. Rev. A **7**, 1648 (1973).
[47] E. R. Davidson, *Reduced Density Matrices in Quantum Chemistry* (Academic Press, New York, 1976).
[48] P. O. Löwdin, Phys. Rev. **97**, 1490 (1955).
[49] T. Ziegler, A. Rauk, and E. J. Baerends, Theoret. Chim. Acta **43**, 261 (1977).
[50] J. Harris, Phys. Rev. A **29**, 1648 (1984).
[51] K. Burke and J.P. Perdew, Mod. Phys. Lett. B **9**, 829 (1995).
[52] K. Burke, J. P. Perdew, and D. C. Langreth, Phys. Rev. Lett. **73**, 1283 (1994).
[53] J. P. Perdew, K. Burke, and Y. Wang, *Real space cutoff construction of a generalized gradient approximation: derivation of the PW91 functional*, in preparation for Phys. Rev.
[54] J.P. Perdew, Int. J. Quantum Chem. **49**, 539 (1994).
[55] H. Yasuhara, Solid State Commun. **11**, 1481 (1972).
[56] M. Taut, Phys. Rev. A **48**, 3561 (1993).
[57] J. P. Perdew and A. Zunger, Phys. Rev. B **23**, 5048 (1981).
[58] R. Colle and O. Salvetti, Theoret. Chim. Acta **37**, 329 (1975).
[59] R. McWeeny, in *The New World of Quantum Chemistry: Proceedings of the Second International Congress of Quantum Chemistry*, eds. B. Pullman and R.G. Parr (Reidel, Dordrecht, 1976).
[60] J.C. Grossman, L. Mitas, and K. Raghavachari, *Structure and stability of molecular carbon: Importance of electron correlation*, preprint
[61] M.A. Buijse and E.J. Baerends, in *Density Functional Theory of Molecules, Clusters, and Solids*, ed. D.E. Ellis (Kluwer Academic Publishers, Amsterdam, 1995).
[62] S.H. Vosko and J.B. Lagowski, in *Density Matrices and Density Functionals*, edited by R.M. Erdahl and V.H. Smith, Jr., (Reidel, Dordrecht, 1986).
[63] N.C. Handy, D.J. Toser, G.J. Laming, C.W. Murray, and R.D. Amos, Isr. J. Chem **33**, 331 (1994).
[64] J.P. Perdew, Phys. Lett. A **165**, 79 (1992).
[65] A. Görling, M. Levy, and J. P. Perdew, Phys. Rev. B **47**, 1167 (1993).
[66] A.D. Becke, unpublished.
[67] R.S. Grev and H.F. Schaefer III, J. Chem. Phys. **96**, 6854 (1992).
[68] P. Fuentealba and A. Savin, Chem. Phys. Lett. **217**, 566 (1994).
[69] H. Stoll, E. Golka, and H. Preuß, Theoret. Chim. Acta **55**, 29 (1980).
[70] E. I. Proynov and D. R. Salahub, J. Chem. Phys. **49**, 7874 (1994).
[71] C. Møller and M. S. Plessett, Phys. Rev. **46**, 618 (1934).
[72] E. Eggarter and T.P. Eggarter, J. Phys. B **11**, 2069 (1978).
[73] E. R. Davidson, S. A. Hagstrom, and S. J. Chakravorty, Phys. Rev. A **44**, 7071 (1991).
[74] K. Jankowski and P. Malinowski, Phys. Rev. A **21**, 45 (1980).
[75] K. Jankowski, P. Malinowski, and M. Polasik, J. Phys. B: Atom. Molec. Phys. **12**, 3157 (1979).
[76] A. K. Rajagopal, J. C. Kimball, and M. Banerjee, Phys. Rev. A **18**, 2339 (1978).
[77] N.W. Ashcroft and N.D. Mermin, *Solid State Physics* (Holt, Rinehart, and Winston, NY, 1976), problem 2 of Chapter 2.
[78] R. Shepard, I. Shavitt, R. M. Pitzer, D. C. Comeau, M. Pepper, H. Lischka, P. G. Szalay, R. Ahlrichs, F. B. Brown, and J.-G. Zhoa, Int. J. Quantum Chem. **142**, 22 (1988).
[79] R. Shepard, H. Lischka, P. G. Szalay, T. Kovar, and M. Ernzerhof, J. Chem. Phys. **96**, 2085 (1992).
[80] *MOLCAS version 2*, 1991, K. Andersson, M. P. Flüscher, R. Lindh, P.-Å. Malmqvist, J. Olsen, B. O. Roos, and A. Sadlej, University of Lund, Sweden, and P.-O. Widmark, IBM Sweden.
[81] A. Szabo and N.S. Ostlund, *Modern Quantum Chemistry* (MacMillan, New York, 1982).
[82] R. Ahlrichs, M. Bär, M. Häser, H. Horn, and C. Kölnel, Chem. Phys. Lett. **94**, 2978 (1992).